

Parametric Design and Optimization of Multi-Rotor Aerial Vehicles

Christos Ampatis and Evangelos Papadopoulos

Abstract. This work addresses the optimal selection of propulsion components for a multi-rotor aerial vehicle (MRAV), for a given payload, payload capacity, number of rotors and flight duration. A steady state model is developed for motors, propellers, electronic speed controllers (ESC), and batteries, using a simplified analysis. Based on technical specifications of batteries, motors and ESCs, component functional parameters are expressed as a function of an equivalent length. Propeller models are developed using experimental data. An optimization program is developed, which calculates the optimal design vector, employing as objective function the energy consumption or the vehicle diameter. Using this program, the influence of the payload and of the number of rotors on the design vector and the MRAV size is studied. The results obtained by the program were compared successfully to existing commercial MRAs.

Keywords: Multi-rotor aerial vehicle (MRAV) design, parametric design, constrained energy and size minimization.

1. INTRODUCTION

Recently, Multi-rotor Aerial Vehicles (MRAV) are encountered in an increasing number of military and civilian applications. A particular advantage an MRAV has over other aerial vehicles is its unique ability for vertical stationary flight (VTOL). Micro and mini MRAs with payload capabilities of up to 100g and 2kg respectively [1], offer major advantages when used for aerial surveillance and inspection in complex and dangerous indoor and outdoor environments. In addition, improvements and availability in cost effective batteries and other technologies, is rapidly increasing the scope for commercial opportunities.

In most MRAV configurations, rotors are in the same plane and symmetrically fixed on the airframe. To balance the torque produced by the rotors, the number of rotors is even. An exception is the trirotor, where one rotor is placed on a tilting mechanism that balances the excess torque. Additional configurations include MRAs with multiple pairs of coaxial – counter rotating rotors, or experimental configurations where the rotors are placed arbitrarily in 3D space [2], or even having the ability of thrust vectoring [3], [4].

Recent studies resulted in optimized designs of micro and

mini rotorcraft vehicle propellers that are easy to manufacture, such as curved plate plastic propellers, [5], [6]. However, in most cases MRAV components come from remotely controlled (RC) aircrafts. Consequently, an MRAV designer would benefit from an automated design method that would take into account all design requirements to yield an optimized combination of commercially available components. Although studies on automated design methods were proposed ([7], [8]), no method that takes into account both the propulsion system and the functional parameters of existing components exists.

In this paper, we propose an MRAV design methodology, which selects the optimum propulsion system components. Given the MRAV design requirements such as payload, payload capacity, number of rotors, and flight duration, a Matlab program calculates the propulsion system components and MRAV size that leads to an energy-efficient design or to a design with the smallest size. To achieve this, we use simplified models for each component and expressions of component functional parameters as a function of component size, using their commercially available technical specifications.

2. COMPONENT AND SYSTEM MODELING

The components to be modeled include motors, electronic speed controllers, batteries, propellers and the airframe. Their simplified models will lead to a MRAV system model.

2.1. Electric Motor Model

The motors used in MRAV applications are Brushless Direct Current (BLDC), due to their high efficiency. Usually, outrunners are used since their high torque constant (K_T) allows direct propeller coupling, unlike with inrunners, which require a gearbox. Although a BLDC is a synchronous 3-phase permanent magnet motor, it can be modeled as a permanent magnet DC motor using a classic three-constant model.

In this model V_k is the supply voltage (V), i_a is the current through the motor coils (A), e_a is the back-electromotive force (EMF) (V), R_a is the armature resistance (Ω) and ω is its shaft angular velocity (rad/s). The motor equations are:

$$V_k = e_a + i_a R_a \quad (1)$$

$$e_a = K_e \omega = K_T \omega = N / K_V \quad (2)$$

where K_e is the motor back EMF constant (Vs/rad), K_T is the motor torque constant (Nm/A), N is the motor rpm, and K_V is motor speed constant (rpm/V). The K_T is related to K_V by:

$$K_e = K_T = 30 / (\pi K_V) \quad (3)$$

The output torque is:

Christos Ampatis is with the Department of Mechanical Engineering, National Technical University of Athens, Greece (e-mail: christos.ampatis@gmail.com).

Evangelos Papadopoulos is with the Department of Mechanical Engineering, National Technical University of Athens, Greece (phone: +30-210-772-1440; fax: +30-210-772-1450; e-mail: egpapado@central.ntua.gr).

$$M_{mot} = K_T (i_a - i_0) \quad (4)$$

where i_0 is the no-load current. The motor input power is:

$$P_{in} = V_k i_a \quad (5)$$

the motor output power is:

$$P_{mot} = M_{mot} \omega = K_T (i_a - i_0) \omega = (V_k - i_a R_a) (i_a - i_0) \quad (6)$$

and the motor speed in rpm is:

$$N = (V_k - i_a R_a) K_V \quad (7)$$

Given K_T , R_a and i_0 a motor's performance is described.

2.2. Electronic Speed Controller Model

Electronic speed controllers regulate motor speed within a range depending on load and battery voltage. The important variable is ESC power loss, caused by its power MOSFETs and transistor drain-to-source "ON" state resistance $R_{DS(ON)}$. The range of $R_{DS(ON)}$ is between 3 and 15 m Ω , and its value depends on transistor size. Considering that ESC power losses are a small portion of input power, and the fact that ESC manufacturers do not include in ESC documentation the type of transistors used, we model the ESC as a constant value resistor of $R_{DS(ON)} = 5$ m Ω . BLDC motor ESCs use three pairs of transistors to manage the three phase currents, so the total resistance of the ESC will be:

$$R_{ESC} = 3R_{DS(ON)} = 0.015\Omega \quad (8)$$

Another important quantity of ESC is the maximum current i_{ESC} they can handle. This appears as a design constraint.

2.3. Battery Model

Due to their high energy density and discharge rate, MRAVs use Lithium Polymer (LiPo) batteries. A LiPo pack consists of identical LiPo cells each with a nominal voltage of 3.7 V. Parallel connection of battery packs raises the battery total capacity, while keeping the nominal total voltage the same. Therefore, the nominal total voltage of a LiPo battery is:

$$V_b = n_c 3.7 \quad (9)$$

where n_c is the number of cells connected in series in a battery pack. The battery has an internal total resistance $R_{bat,tot}$. When connected to a load its output voltage is:

$$V_{b,out} = V_b - i R_{bat,tot} \quad (10)$$

where i is the battery load current.

Each cell has internal resistance R_{sc} , power P_{sc} , and energy E_{sc} . To calculate $R_{bat,tot}$ we apply Kirchoff's laws to a battery consisted of n_p identical packs connected in parallel, each of which consists of n_c identical cells connected in series. Each battery pack has an internal resistance:

$$R_i = n_c R_{sc}, \quad i = 1, \dots, n_p \quad (11)$$

The battery total resistance is:

$$R_{bat,tot} = \prod_{j=1}^{n_p} R_j \left/ \sum_{i=1}^{n_p} \left(\frac{1}{R_i} \prod_{j=1}^{n_p} R_j \right) \right. = \frac{n_c R_{sc}}{n_p} \quad (12)$$

A battery's total power is:

$$P_{bat,tot} = P_{sc} n_c n_p \quad (13)$$

while its total energy is:

$$E_{bat,tot} = E_{sc} n_c n_p \quad (14)$$

2.4. Propeller Model

Propellers used on MRAVs are mostly the same propellers used in remote controlled (RC) airplanes. Propeller performance is described by its thrust T (N), power P (W) and torque M (Nm). To model performance in static conditions, we use manufacturer data such as propeller diameter D_p and its pitch p at 75% of its radius. Performance quantities are then related to propeller speed, diameter and pitch. This is achieved through a number of coefficients.

The thrust coefficient is given by:

$$C_T = T / \rho (N/60)^2 D^4 \quad (15)$$

where T is thrust (N), ρ is air density (kg/m³), N is propeller speed (rpm), and D is propeller diameter (m).

The power coefficient is given by:

$$C_P = 2\pi C_M = P / \rho (N/60)^3 D^5 \quad (16)$$

where P is power (W) and C_M the torque coefficient.

These coefficients are next related to propeller diameter and pitch. Using the Blade Element Momentum Theory (BEMT) and a series of mild assumptions [9], we get the following equations for thrust and power coefficients:

$$C_T = \frac{\pi^3}{4} \frac{1}{2} \sigma C_{la} \left(\frac{\theta_{0.75}}{3} - \frac{1}{2} \sqrt{\frac{4}{\pi^3} \frac{C_T}{2}} \right) \quad (17)$$

$$C_P = \frac{2}{\pi^2} \frac{C_T^{3/2}}{\sqrt{2}} + \frac{1}{8} \sigma C_{d0} \quad (18)$$

where σ is propeller solidity, C_{la} is the slope of blade airfoil lift coefficient – incidence angle curve, $\theta_{0.75}$ is propeller pitch angle at 75% of the propeller radius R , and C_{d0} is a blade airfoil drag coefficient for zero lift.

To further simplify this model to a restricted propeller size range and geometry, we make the following assumptions. Considering that we refer to geometrically scaled propellers, propeller solidity σ will be constant regardless of propeller size. Additionally, if the propeller size range is no more than one order of magnitude, then the Reynolds number does not change dramatically, so we can assume that the aerodynamic quantities C_{la} and C_{d0} are constant. Consequently, thrust and power coefficients are only a function of propeller pitch angle $\theta_{0.75}$. Pitch angle $\theta_{0.75}$ is related to propeller pitch $p_{0.75}$ as:

$$\theta_{0.75} = \arctan(4 / 3\pi \cdot p_{0.75} / D_p) \quad (19)$$

Consequently, using (17), (18) and (19) we can relate C_T and C_P to the ratio $p_{0.75}/D_p$ only. Normally, $\theta_{0.75}$ is in the range of 5° to 30°, resulting a $p_{0.75}/D_p$ range of 0.2 to 1.35. In this region the function $C_T(p_{0.75}/D_p)$ is linear and this can be shown through a numerical solution. Additionally, by observing (18) we see that C_P is proportional to $C_T^{3/2}$, therefore it is proportional to $(p_{0.75}/D_p)^{3/2}$, and this can be also shown through a numerical solution in the $p_{0.75}/D_p$ range. The simplified expressions for thrust and power coefficients are:

$$C_T = k_1 (p/D_p) + k_2 \quad (20)$$

$$C_p = k_3 \left(p/D_p \right)^{3/2} + k_4 \quad (21)$$

where constants k_1 to k_4 can be calculated using experimental data of geometrically scaled propellers.

2.5. System Model

The system model results from the combination of the propulsion system model and the equilibrium of forces acting on the vehicle. The propulsion system consists of the battery and n_{mot} triples of ESC, and of the motors and propellers connected in parallel.

The physical model of the propulsion system shown in Fig. 1, combines each component model and outputs the total thrust produced by the n_{mot} rotors. If all rotors have the same speed, the current drawn will be the same for each one.

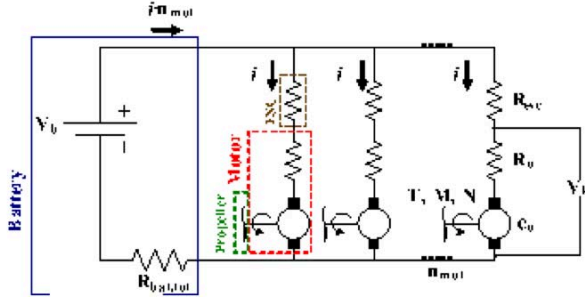


Fig. 1 Propulsion system physical model.

Applying Kirchoff's law to the circuit of Fig. 1 we get:

$$V_k + iR_{ESC} = V_b - n_{mot}iR_{bat,tot} \quad (22)$$

$$e_a = V_b - i(R_a + R_{ESC} + n_{mot}R_{bat,tot}) \quad (23)$$

The rotor speed is given by:

$$N = \left[V_b - i(R_a + R_{ESC} + n_{mot}R_{bat,tot}) \right] K_V \quad (24)$$

The above equation is valid only at full throttle, when the ESC transistors are fully on; otherwise, at partially open throttle the ESC output voltage is less than the maximum, thus the motor voltage will be less than V_k .

Eq. (24) shows that the motor equivalent resistance is:

$$R_{tot} = R_a + R_{ESC} + n_{mot}R_{bat,tot} \quad (25)$$

If i_0 is the no-load current, then the maximum speed is:

$$N_{max} = \left[V_b - i_0R_{tot} \right] K_V \quad (26)$$

In this paper we examine the case where the vehicle during a total flight time t_{tot} has two operational modes. (a) A *maximum thrust mode* for a percentage ATP of the total flight time t_{tot} , in which motors are at full throttle state producing the maximum static thrust, and (b) a *hover mode*, in which the vehicle hovers for the rest of the flight time.

(a) Maximum thrust mode: The rotor speed is:

$$N_{acc} = \left[V_b - i_{acc}R_{tot} \right] K_V \quad (27)$$

which is equivalent to the following:

$$N_{acc} = \left[V_{k,acc} - i_{acc}R_a \right] K_V \quad (28)$$

where $V_{k,acc}$ is the motor supply voltage equal to the maximum ESC output voltage.

The vehicle has the ability to accelerate with an instantaneously maximum acceleration a , therefore it has the ability to lift its total weight f_w times, thus:

$$a = (f_w - 1)g \quad (29)$$

A balance of forces yields:

$$\begin{aligned} \Sigma F &= m_{tot}a \Rightarrow n_{mot}T_{acc} - m_{tot}g = m_{tot}a = (f_w - 1)m_{tot}g \\ &\Rightarrow n_{mot}C_T\rho(N_{acc}/60)^2 D_p^4 = f_w m_{tot}g \end{aligned} \quad (30)$$

The total mass of the vehicle is:

$$m_{tot} = m_{bat,tot} + (m_{mot} + m_p + m_{ESC})n_{mot} + m_{frm} + m_{pl} \quad (31)$$

where, $m_{bat,tot}$ is the battery total mass, m_{mot} is the motor mass, m_p is the propeller mass, m_{ESC} is the ESC mass, m_{frm} is the airframe mass, and m_{pl} is the payload mass.

The motor – propeller torque balance yields:

$$M_m = M \Rightarrow K_T(i_{acc} - i_0) = C_P\rho(N_{acc}/60)^2 D_p^5 / 2\pi \quad (32)$$

The system input power is:

$$P_{IN,acc} = V_b i_{acc} n_{mot} \quad (33)$$

while the system energy consumption is:

$$E_{IN,acc} = P_{IN,acc} ATP \quad (34)$$

(b) Hover mode: In this mode, the motor speed is:

$$N_{hov} = \left[V_{k,hov} - i_{hov}R_a \right] K_V \quad (35)$$

where $V_{k,hov}$ is ESC output voltage that satisfies $V_{k,hov} < V_{k,acc}$.

The balance of forces yields:

$$\Sigma F = 0 \Rightarrow n_{mot}T_{hov} = m_{tot}g \Rightarrow \quad (36)$$

$$n_{mot}C_T\rho(N_{hov}/60)^2 D_p^4 = m_{tot}g$$

The motor – propeller torque balance gives:

$$M_m = M \Rightarrow K_T(i_{hov} - i_0) = C_P\rho(N_{hov}/60)^2 D_p^5 / 2\pi \quad (37)$$

The system input power is:

$$P_{IN,hov} = V_b i_{hov} n_{mot} \quad (38)$$

and the system energy consumption is:

$$E_{IN,hov} = P_{IN,hov} t_{tot} (1 - ATP) \quad (39)$$

while the total input energy is given by:

$$E_{IN,hov} + E_{IN,acc} = E_{tot} \quad (40)$$

3. PARAMETERIZATION

The system equations depend on functional parameters, which define system response. Here, these parameters are expressed as a function of component length, taken as the cubic root of a component's volume (cubic length), referred to as the *equivalent length*. We do the same with propellers using available experimental data. Furthermore, using rational geometric considerations and strength of materials theory, equations that correlate airframe size and mass as a function of propeller diameter, number of rotors and maximum thrust, ensuring airframe durability and its ability to accommodate electronics and batteries, were developed [10].

3.1. Electric Motor

The electric motors we chose for parameterization are the outrunner BLDC motors from manufacturer AXI. The

choice based on the technical specifications availability, and on the performance of these motors.

Here, the equivalent length of each motor is related to the outer dimensions of the motor, and not to its stator dimensions. The parameters we want to relate to the equivalent length are the motor armature resistance R_a , torque constant K_T , no load current i_0 , and motor mass m_{mot} . Additionally, motor maximum sustained current (or current capacity) i_{max} , and motor maximum speed $N_{m,max}$, are parameters that limit motor performance and must be related to equivalent length.

After investigation of various correlations of these parameters to the equivalent length, we concluded the following functions due to their optimal fit to manufacturer data. Below, R^2 refers to coefficient of determination, and l_{mot} to motor equivalent length (m).

$$K_T/R_a = 2.6533 \cdot 10^4 l_{mot}^{3.6032}, R^2 = 0.902 \quad (41)$$

$$K_T^2/R_a = 1.7548 \cdot 10^5 l_{mot}^{5.4833}, R^2 = 0.94 \quad (42)$$

$$M_0 = K_T i_0 = 5.7721 \cdot 10^2 l_{mot}^{3.1888}, R^2 = 0.908 \quad (43)$$

$$M_{max} = K_T (i_{max} - i_0) = 4.5004 \cdot 10^5 l_{mot}^{4.2222}, R^2 = 0.96 \quad (44)$$

$$N_{m,max} = (n_{c,max} 3.7 - i_0 R_a) K_V \Rightarrow$$

$$N_{m,max} = 25604 e^{-17.687 l_{mot}}, R^2 = 0.35 \quad (45)$$

where, $n_{c,max}$ is the maximum number of battery cells in series connection that is proposed by manufacturer.

To relate motor mass to motor equivalent length, we calculated the mean motor density $\rho_{mot} = 2942 \text{ kg/m}^3$.

3.2. Electronic Speed Controller

We chose to parameterize ESCs from JETI due to the availability of technical specifications and their performance. Although the ESC is modeled as a constant resistance, additional parameters are needed that relate its operational limit and mass properties to its equivalent length l_{ESC} (m). These parameters are the ESC maximum sustained current i_{ESC} , and ESC mean density ρ_{ESC} . Using ESC specifications, correlations of maximum sustained current i_{ESC} and ESC equivalent length l_{ESC} are obtained as:

$$i_{ESC} = 8.4545 \cdot 10^6 l_{ESC}^{3.2451}, R^2 = 0.88 \quad (46)$$

The mean ESC density calculated as $\rho_{ESC} = 2580 \text{ kg/m}^3$.

3.3. Battery

We chose to parameterize batteries from Kokam for the same reasons as before. The parameters to be related to battery total equivalent length l_{bat} include total power $P_{bat,tot}$, total energy $E_{bat,tot}$, total resistance $R_{bat,tot}$ and mass m_{bat} .

Battery specifications concern single 3.7V battery cells. However, we need information for any combination of parallel and series connected cells. We assume that n_p cells connected in parallel result in a larger single cell with volume B_{vol} , power P_{bat} , energy E_{bat} , and internal resistance R_{bat} .

Assuming that the battery consists of $n_p n_c$ identical cells of volume $B_{vol,sc}$ each, then an equivalent battery will consist of n_c equivalent cells each of which has volume:

$$B_{vol} = n_p B_{vol,sc} \quad (47)$$

Therefore, each equivalent cell volume will be:

$$B_{vol} = l_{bat}^3 / n_c \quad (48)$$

Applying curve fitting to manufacturer data, the following equation for single cell internal resistance was obtained:

$$R_{sc} = 2.84668 \cdot 10^{-7} B_{vol,sc}^{-0.951154}, R^2 = 0.95 \quad (49)$$

Correspondingly, the equivalent cell internal resistance is:

$$R_{bat} = 2.84668 \cdot 10^{-7} B_{vol}^{-0.951154} \quad (50)$$

Using (12), (49) and (50), the battery total resistance is:

$$R_{bat,tot} = n_c R_{sc} / n_p = n_c 2.84668 \cdot 10^{-7} (B_{vol} / n_p)^{-0.951154} / n_p \Rightarrow$$

$$R_{bat,tot} = n_c R_{bat} n_p^{-(1-0.951154)} \approx n_c R_{bat} n_p^{-0.05} \quad (51)$$

However, n_p will never be large, therefore using the approximation $n_p^{0.05} \approx 1$, battery total resistance will be:

$$R_{bat,tot} = n_c R_{bat} \quad (52)$$

Applying curve fitting to manufacturer data, we observe that cell energy and power are proportional to its volume. Therefore, using the mean value of the ratios cell energy to cell volume and cell power to cell volume, we can calculate the battery total power and energy as:

$$P_{bat,tot} = n_c P_{bat} = n_c 7.0899 \cdot 10^6 B_{vol} \quad (53)$$

$$E_{bat,tot} = n_c E_{bat} = n_c 9.0833 \cdot 10^8 B_{vol} \quad (54)$$

The mean battery cell density is found as $\rho_{bat} = 1907.8 \text{ kg/m}^3$.

3.4. Propeller

The propellers we chose to parameterize are taken from APC. The parameters to be related to propeller diameter D_p and geometric pitch p , are the thrust and power coefficient, C_T and C_P respectively. Previously, it was shown through Eqs. (20) and (21), that for zero flight velocity, C_T and C_P are functions of the ratio p/D_p . The constants k_1 through k_4 in these equations depend on propeller design and the Reynolds number. Here, we are interested in propellers with diameter of 80 mm to 500 mm, therefore we use experimental data for these dimensions, so as to satisfy Reynolds number.

Experiments on commercially available propellers used in remote controlled aircrafts, were conducted at the University of Illinois, Urbana-Champaign (UIUC) in a wind tunnel [11]. Here, data regarding SPORT type APC propellers are used. From the C_T and C_P measurements for these propellers, those that refer to static conditions are used here. We observed that C_T and C_P are not affected much by propeller speed; therefore we calculated mean values of C_T and C_P for various speeds. These measurements concern propeller diameter of 7 in to 14 in. Finally, the C_T and C_P were correlated to the ratio p/D_p , obtaining the following functions:

$$C_T = 0.0266 (p / D_p) + 0.0793, R^2 = 0.31 \quad (55)$$

$$C_P = 0.0723 (p / D_p)^{3/2} + 0.0213, R^2 = 0.83 \quad (56)$$

The propeller mass is related to propeller diameter D_p as:

$$m_p = 0.97573 D_p^{2.5741}, R^2 = 0.98 \quad (57)$$

4. COMPONENT OPTIMAL SELECTION

In the previous sections, component performance was related to its equivalent length. Next, a method is developed for the optimal lengths selection, which are parameters of the design vector. This vector minimizes an objective function, which is either the vehicle total energy, or the vehicle diameter D_{rob} .

4.1. Design Parameters

The design requirements are described by a number of parameters set by the designer. These include the payload m_{pl} , the total flight time t_{tot} , the payload capacity described by f_w indicating how many times the vehicle can lift its own weight, and the factor ATP which indicates the percentage of total flight time that the vehicle is at maximum thrust mode.

The design vector consists of the number of battery cells n_c in series, the equivalent battery length l_{bat} , the equivalent motor length l_{mot} , the equivalent ESC length l_{ESC} , the propeller diameter D_p , the ratio p/D_p , and the number of rotors n_{mot} .

The design vector domain results from the size limits of the components that were parameterized earlier. Outside these regions the functions developed earlier may not apply.

4.2. Calculation Procedure

In every optimization step, the requirements vector (m_{pl} , t_{tot} , f_w , ATP) is constant, while the design vector (n_c , l_{bat} , l_{mot} , l_{ESC} , D_p , p/D_p , n_{mot}) changes until the minimization of objective function is reached.

The calculation procedure follows the following sequence. At first, components quantities are calculated using (41) through (57). The battery nominal voltage V_b is calculated using (9). For the maximum thrust mode, using (30) we calculate the speed N_{acc} , then from (32) we get the motor current i_{acc} , and using (28) we calculate motor voltage $V_{k,acc}$. The motor maximum speed is calculated using (26). Next, using (33), the maximum total input power $P_{IN,acc}$ is calculated, while using (34) we find the total input energy at maximum thrust mode $E_{IN,acc}$. For the hover mode, and using (36), we calculate the speed N_{hov} . Then from (37) we get the motor current i_{hov} , and using (35) we calculate motor voltage $V_{k,hov}$. The total input energy at hover $E_{IN,hov}$ is obtained using (39), while the total input energy E_{tot} is found using (40).

4.3. Constraints

The constraints result from independent variable physical consistency. They are given as follows:

$$\begin{aligned} V_{acc} - V_b &\leq 0, & N_{acc} - N_{max} &\leq 0, & i_{max} - i_{ESC} &\leq 0 \\ i_{acc} - i_{max} &\leq 0, & i_{hov} - i_{acc} &\leq 0, & P_{IN,acc} - P_{bat,tot} &\leq 0 \\ E_{tot} - E_{bat,tot} &\leq 0, & -i_{acc} &\leq 0, & -i_{max} &\leq 0 \end{aligned} \quad (58)$$

4.4. Optimization Methodology

For the calculation procedure, a Matlab program was developed that employs the ‘fmincon’ function (minimum of constrained nonlinear multivariable function), which uses one target deterministic constrained optimization method for non-linear multivariable objective function. Our targets were to determine the most energy efficient design, or the smallest one. Hence, the objectives were the minimization of battery energy $E_{bat,tot}$ or vehicle diameter D_{rob} , respectively.

In order to check that ‘fmincon’ would not be trapped in local minima, we also developed a program that scans the whole design vector domain, using nested loops. We observed no differences between these methods after a number of test runs. Consequently, we considered that ‘fmincon’ calculates the absolute minimum for our objective functions.

5. DESIGN SCENARIOS

Using the calculation procedure described in Section 0, some test runs are carried out to study the influence of payload and number of rotors on the design vector and the MRV size. In all scenarios, the requirement parameters are set to: $t_{tot}=15$ min, $f_w=2$, $ATP=0.1$. Finally, we compare our program results to commercially available MRVs designs.

5.1. Study of the Parametric Influence

Payload influence. The payload changes from zero to 1.5kg, while the number of rotors is 4 and constant. In Fig. 2, the payload influence on the design vector is shown; F_{obj} is the objective function, D_{rob} is the vehicle total diameter, and E_{tot} is the battery total energy. We observe that as the payload increases, the equivalent length increases due to power increase. Also, minimizing energy yields a more efficient but larger design than that obtained by minimizing vehicle size.

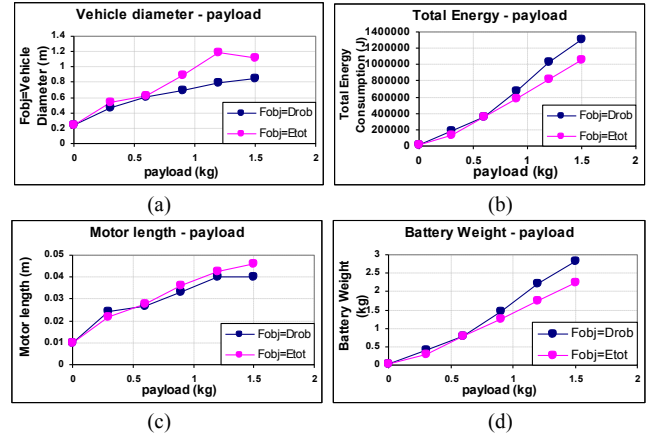


Fig. 2 Influence of payload on: (a) Vehicle diameter, (b) Total energy, (c) Motor length, (d) Battery weight, for 4 rotors.

Observing the battery mass chart, we can say that battery mass is always lower for the minimization of total energy. Additionally, we can see that battery mass increases linearly with payload. For the quadrotor, we can say that we need 1.5 kg of batteries for 1 kg payload; since the flight time is 15 min, then we can say that for 1 kg payload we need 100 gr batteries for every minute of flight.

Number of rotors influence. The number of rotors changes from 3 to 8, while the payload is constant and equal 1kg. In Fig. 3, the influence of rotor number on the design vector is presented. We observe that for energy minimization, the best design has 8 rotors, but this is true for a payload of 1kg, see Fig. 4. We observe also the expected decrease in component equivalent length when the number of rotors increases. Additionally, the designer can further enrich the optimization procedure by adding a look-up table of discrete component values available on the market, as described in [12].

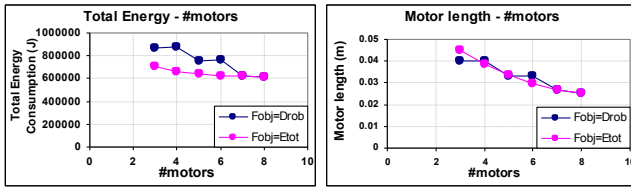


Fig. 3 Influence of number of rotors on the design vector for payload equal to 1kg. Objective functions comparison.

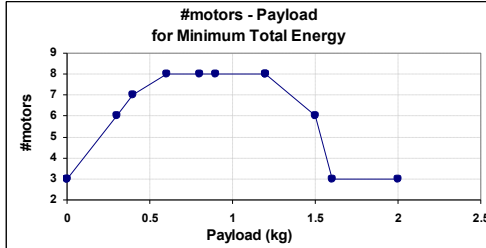


Fig. 4 Influence of payload on the number of rotors for minimum energy.

Hence, a second optimization using this table and the results obtained by the proposed methodology will designate the exact components.

5.2. Test Cases

Using the developed design methodology we can produce designs for various MRV configurations. However, to determine whether this methodology is valid and yields designs close to reality, we compare program results to two existing commercial MRVs. The first is the quadrotor Walkera HM Hoten X Quadcopter, a small MRV designed for a payload less than 100 gr. The other is the Octocopter X88-J2, a large MRV designed for aerial photography and for payloads up to 1.5 kg.

Table I presents the quadrotor comparison, with data retrieved from [13]. The 0.1 kg payload includes the electronics and control unit. Payload capacity is $f_w=2$, $ATP=0.1$ and total flight time is 10 min. We observe that the program yields results very close to reality. The difference lies on battery configuration and mass. The actual vehicle uses two battery cells in series, and with total energy $2 \cdot 3.7V \cdot 1Ah = 7.4Wh$, while the optimized one needs $1 \cdot 3.7V \cdot 1.611Ah = 6Wh$. Therefore, the optimized vehicle appears to be more energy-efficient.

In Table II, an octocopter comparison is presented, with data taken from [14]. The payload is 1.13 kg, payload capacity

Table I. Optimized and actual Walkera Quadcopter comparison.

Model	Walkera Hoten X Quadcopter	Optimization	Difference
Total mass (kg)	0.332	0.283	-0.05
Battery Capacity (Ah)	1	1.6	0.6
Battery #cells	2	1	-1
Battery mass (kg)	0.064	0.046	-0.02
Propeller diameter (m)	0.186	0.184	0.00
Vehicle diameter (m)	0.500	0.510	0.01

Table II. Optimized and actual Octocopter X88-J2 comparison.

Model	X88-J2 Octocopter	Optimization	Difference
Total mass (kg)	3.11	3.23	0.12
Battery Capacity (Ah)	10.6	21.4	10.8
Battery #cells	4	2	-2
Battery mass (kg)	1.11	1.22	0.11
Propeller diameter (m)	0.305	0.24	-0.07
Vehicle diameter (m)	1.205	0.91	-0.29

is $f_w=1.51$), $ATP=0.1$ and the total flight time is 17.5 min. Observe that the optimized vehicle is 8% heavier but 25% smaller. Also, the optimized vehicle batteries have twice the capacity because there are two battery cells in series. Thus, the total energy of the optimized vehicle is $2 \cdot 3.7V \cdot 21.43Ah = 159Wh$, while that of the actual vehicle is $4 \cdot 3.7V \cdot 10.6Ah = 157 Wh$; i.e. the energy is almost the same in both designs.

6. CONCLUSIONS

This work focused on the parametric design and optimization of a multi-rotor aerial vehicle (MRV). Using simplified models of propulsion components, a system model for an MRV was created and performance at hovering and at maximum thrust was described. Based on technical specifications of batteries, motors and ESCs, component functional parameters were expressed as a function of equivalent lengths. Propeller models were developed using experimental data. An optimization program was developed which calculates the optimal design vector employing as objective function the energy consumption and vehicle diameter. Using this program, the influence of the payload and of the number of rotors on the design vector and the MRV size was studied. The results obtained by the program were compared to existing commercial MRVs, showing that the developed methodology yields designs close to reality. In addition, it provides an MRV designer with tools to improve existing designs, or create new ones.

REFERENCES

- [1] Kendoul, F., "Survey of advances in guidance, navigation, and control of unmanned rotorcraft systems", *Journal of Field Robotics* Volume 29, Issue 2, March/April 2012, pp. 315–378.
- [2] Jiang, Q. et al, "Analysis and Synthesis of Multi-Rotor Aerial Vehicles", *Proceedings of the ASME 2011 International Design Engineering Technical Conferences & Computers and Information in Engineering Conference*, IDETC/CIE 2011, August 28–31, 2011, Washington, DC, USA, DETC2011-47114.
- [3] Langkamp, D., et al, "An engineering development of a novel hexrotor vehicle for 3D applications", *Proceedings Micro Air Vehicles Conference 2011, Summer edition*.
- [4] Fernandes, N., "Design and construction of a multi-rotor with various degrees of freedom", *M.S. Thesis*, Technical Univ. of Lisboa, 2011.
- [5] Bohorquez, F., et al, "Design, Analysis and Hover Performance of a Rotary Wing Micro Air Vehicle", *Journal of the American Helicopter Society*, Volume 48, Number 2, 1 April 2003, pp. 80-90.
- [6] Harrington, A., "Optimal Propulsion System Design for a Micro Quad Rotor", *M.S. Thesis*, University of Maryland, 2011.
- [7] Lundström, D., Amadori, K., Krus, P., "Automation of Design and Prototyping of Micro Aerial Vehicle", *AIAA-2009-629, 47th AIAA Aerospace Sciences Meeting*, Orlando, FL, USA, Jan. 2009.
- [8] Bouabdallah, S., "Design and Control of Quadrotors with Application to Autonomous Flying", *Ph.D. Thesis*, EPFL, 2007.
- [9] Leishman, J.G., "Principles of Helicopter Aerodynamics", Cambridge University Press, New York, 2006.
- [10] Ampatis, C. "Parametric Design & Optimization of Multicopter Robots," *M.S. Thesis*, Mechanical Eng. Dept., NTUA, 2013 (in Greek).
- [11] Brandt, J. and Selig, M., "Propeller Performance Data at Low Reynolds Numbers", *49th AIAA Aerospace Sciences Meeting*, 2011, AIAA 2011-1255. <http://www.ae.illinois.edu/m-selig/props/propDB.html>.
- [12] E. Papadopoulos, and I. Davliakos, "A Systematic Methodology for Optimal Component Selection of Electrohydraulic Servosystems," *International Journal of Fluid Power*, vol. 5, No. 2, pp. 15-24, 2004.
- [13] Walkera HM Hoten X Quadcopter - 200 size, <http://www.helifreak.com/showthread.php?t=452889>.
- [14] X88-J2 Octocopter, <http://www.wowhobbies.com/x88octocopter.aspx>.